Effect of nanostructured support on the WGSR activity of Pt/CeO_2 catalysts

L. Torrente-Murciano[*1], and F.R. Garcia-Garcia[2]

[1] *Department of Chemical Engineering, University of Bath, Bath, BA2 7AY, UK*
[2] *School of Chemical Engineering and Advanced Materials, Newcastle University, Newcastle upon Tyne, NE1 7RU, UK*

***Keywords*:** water gas shift reaction, platinum, ceria, nanostructured, rods, selectivity

1. Introduction

Hydrogen is widely recognised as a key component in our current search for a renewable and sustainable energy sector. Its conversion in fuel cells in both mobile and stationary applications can provide clean and efficient transportation fuel and electricity. However, highly-pure hydrogen is required as feedstock for fuel cells to avoid the poisoning of the electrodes and its consequent irreversible loss of activity [1]. In the last decade, there has been significant increase in interest in the water gas shift reaction (WGSR) for the production of CO-free hydrogen at temperatures (100-180ºC) relevant to the fuel cell technology [2, 3]. Hydrogen produced by the reforming of hydrogen-rich fuels such as natural gas, methanol or gasoline can contain up to ~10-15% carbon monoxide [4, 5], and the WGSR is presented as a pathway for its removal while increasing the overall hydrogen yield.

Conventional commercial low temperature shift catalysts based on $Cu/ZnO/Al_2O_3$ materials [6] present insurmountable limitations, namely low activity at the relevant fuel cell temperature range, pyrophoric nature and weak stability under cyclic operation. Alternatively, noble metals (Pt, Au, Pd) supported on reducible oxides such as CeO_2 or TiO_2 have been widely presented as highly active and stable WGSR catalysts [7-9]. The reducibility of the surface oxygen of

[*] Corresponding author: Laura Torrente-Murciano, Phone: +44 1225 38 5857, Fax: +44 1225 38 5713
Email: ltm20@bath.ac.uk

ceria was long ago discovered to be greatly promoted by the addition of platinum to its surface [10] with a consequent enhancement of its WGSR activity. Flytzani-Stephanopoulos's group more recently demonstrated that the active sites for the WGSR are platinum species diffused in the subsurface layers of ceria [11], which weaken the surface Ce-O bond, making this oxygen reactive at lower temperatures [12, 13]. The mechanism of formation of these active Pt-Ce-O active species seems to strongly depend on the preparation method as well as being highly sensitive to the ceria structure, even when the metal crystallite size remains constant [14]. Furthermore, addition of dopants into the ceria have been demonstrated to modify the Pt-support interaction and consequently the resulting WGSR activity, having a direct effect on the reaction mechanism [15, 16]. We have recently demonstrated that the oxygen storage capacity and low temperature reducibility of the ceria can be tuned by varying its morphology at the nano-scale by selectively exposing different crystal planes [17], leading to further studies by other groups [18, 19]. In this paper, we demonstrate the relationship between the surface chemical and physical properties of nanostructured ceria and the resulting platinum-support interaction, reducibility of ceria and consequently, WGSR activity, providing relevant insights for future catalyst design in this field.

2. Experimental

Nanostructured ceria with different nano-morphologies were selectively synthesised by varying the conditions during hydrothermal treatment using $Ce(NO_3)_3 \cdot 6H_2O$ as a precursor [17]. Ceria nanorods were synthesised at 100ºC in a 15 M NaOH solution while ceria nanocubes were formed at 180ºC in a 15 M NaOH medium as described elsewhere [20]. Commercial ceria nanoparticles (Sigma) were also used for comparison purposes. Platinum was supported by incipient wetness impregnation at room temperature using a commercial 8% H_2PtCl_6 aqueous

solution (pH = 3) as a metal precursor. Catalysts were dried under vacuum at 80ºC and reduced during 2 hours under 20 mL/min hydrogen flow at 200ºC.

N_2 adsorption analysis at 77 K were carried out using a Micromeritics ASAP 2020. The morphology of the ceria materials and the platinum nanoparticle size distribution was determined with a JEOL TEM-2100 200 kV transmission electron microscope. CO pulse chemisorption analyses at 35°C were carried out using a Micromeritics Autochem II equipment equipped with a thermal conductivity detector (TCD) after sample reduction under hydrogen flow at 200 ºC followed by a pre-treatment at 300 ºC under helium flow. The same equipment was used for the temperature programmed reduction experiments using 5% H_2/Ar with a ramp rate of 10 ºC min^{-1}. The first TPR cycle was performed without any prior-treatment of the sample while 20 mL/min of helium were flown at room temperature during 10 minutes between consecutive temperature programmed experiments.

The water gas shift reaction catalytic activity of the nanostructured 1.5%Pt/CeO_2 catalysts was studied in a differential fixed-bed reactor at atmospheric pressure where 35 mg of catalyst were diluted in SiC to a total 4 cm^3 volume and packed into a 6 mm ID ceramic tube. The reactant gas mixture (100 mL min^{-1}) consisted of Ar (90%), CO (5%) and H_2O vapour (5%) with a GHSV of 4520 h^{-1}. The outlet reaction stream was analysed by on-line gas chromatography equipped with a TCD detector (Varian-3900). Each analysis was repeated three times with an associated experimental error < 5%.

3. Results and discussion

Three nanostructured ceria materials (nanorods, nanocubes and nanoparticles) with different physical properties were used in a series of Pt/CeO_2 catalysts. In all cases, the platinum amount was fixed to 1.5 wt.%, loaded by wetness impregnation. Ceria nanorods present diameters of ~ 7 nm and lengths in the range of 20 – 80 nm and a surface area of 74 m^2 g^{-1}, enclosing (110)

and (100) facets. Ceria nanocubes present bigger dimensions, with sizes from 20 to 100 nm and relatively small surface area (13 m^2 g^{-1}), enclosing (100) facets. Ceria nanoparticles have the highest surface area amongst the materials studied here (144 m^2 g^{-1}) with dimensions ~ 5nm, enclosing (111) and (100) facets. Full physical characterisation of these materials is published elsewhere [17].

The activity of the different Pt/CeO_2 catalysts for the WGSR as a function of temperature is shown in Figure 1A. Carbon monoxide conversion increases as the temperature increases, reaching a plateau (or even decreasing in the case of the 1.5wt.%Pt/ CeO_2 rods) at high reaction temperatures due to thermodynamic limitations.

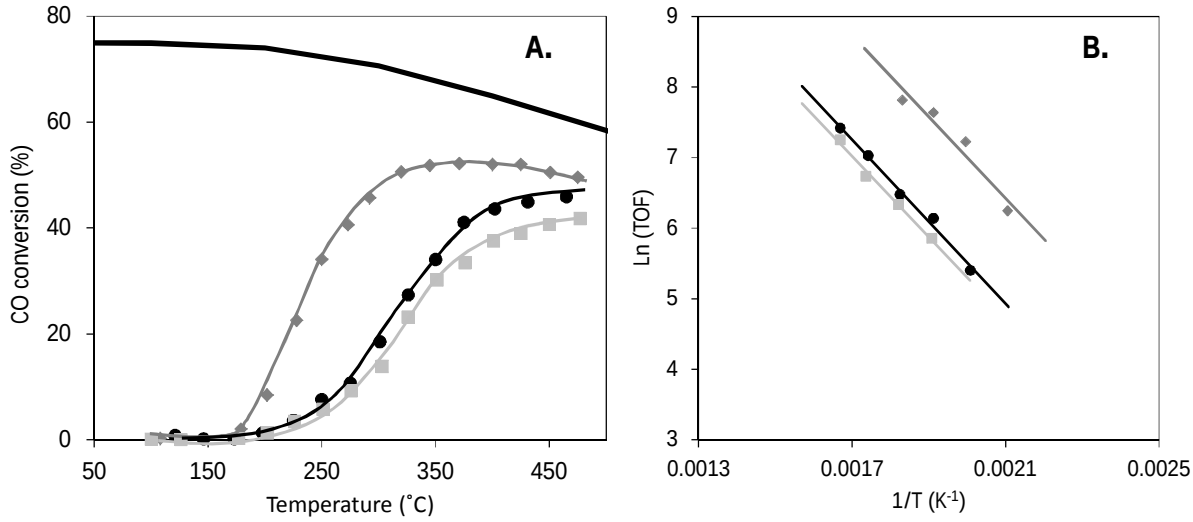

Figure 1: A. WGS activity of 1.5wt.% Pt/nanostructured ceria as a function of reaction temperature. B Arrhenius plot where specific rate values are expressed in mol CO converted · mol Pt · h^{-1} ♦ Pt/CeO_2 nanorods ■ Pt/CeO_2 nanocubes ● Pt/CeO_2 nanoparticles. Solid line represents the thermodynamic equilibrium.

The 1.5wt.% Pt/CeO_2 rods catalyst presents not only higher activity with respect to the 1.5wt.% Pt/CeO_2 cubes and 1.5wt.% Pt/CeO_2 particles, but also reactivity at considerable lower temperatures (180ºC). It is important to highlight that lowering the reaction temperature has a direct impact on the energy efficiency and yield of the final hydrogen production process and

CO removal application. The 1.5wt.% Pt/CeO_2 cubes and 1.5wt.% Pt/CeO_2 particles present water gas shift activity at temperatures >225 ºC with the latter showing a slightly higher activity within the studied temperature range. Comparison of these catalysts to those reported in the literature proved to be difficult due to the variations on the experimental conditions amongst studies, specifically the inlet H_2O/CO ratio which affects not only the thermodynamic equilibrium but also the rate of re-oxidation of ceria.

Figure 2 shows representative TEM images of the Pt/CeO_2 catalysts. None of the ceria materials undergo morphological transformation upon the loading of the platinum or their reduction showing the same morphology and dimensions than the fresh ceria materials [17]. The three catalysts present platinum nanoparticles with sizes < 2nm, some of them indicated by arrows in Figure 2, without the presence of metal agglomerations. No accurate particle size distributions were achieved due to the small platinum size.

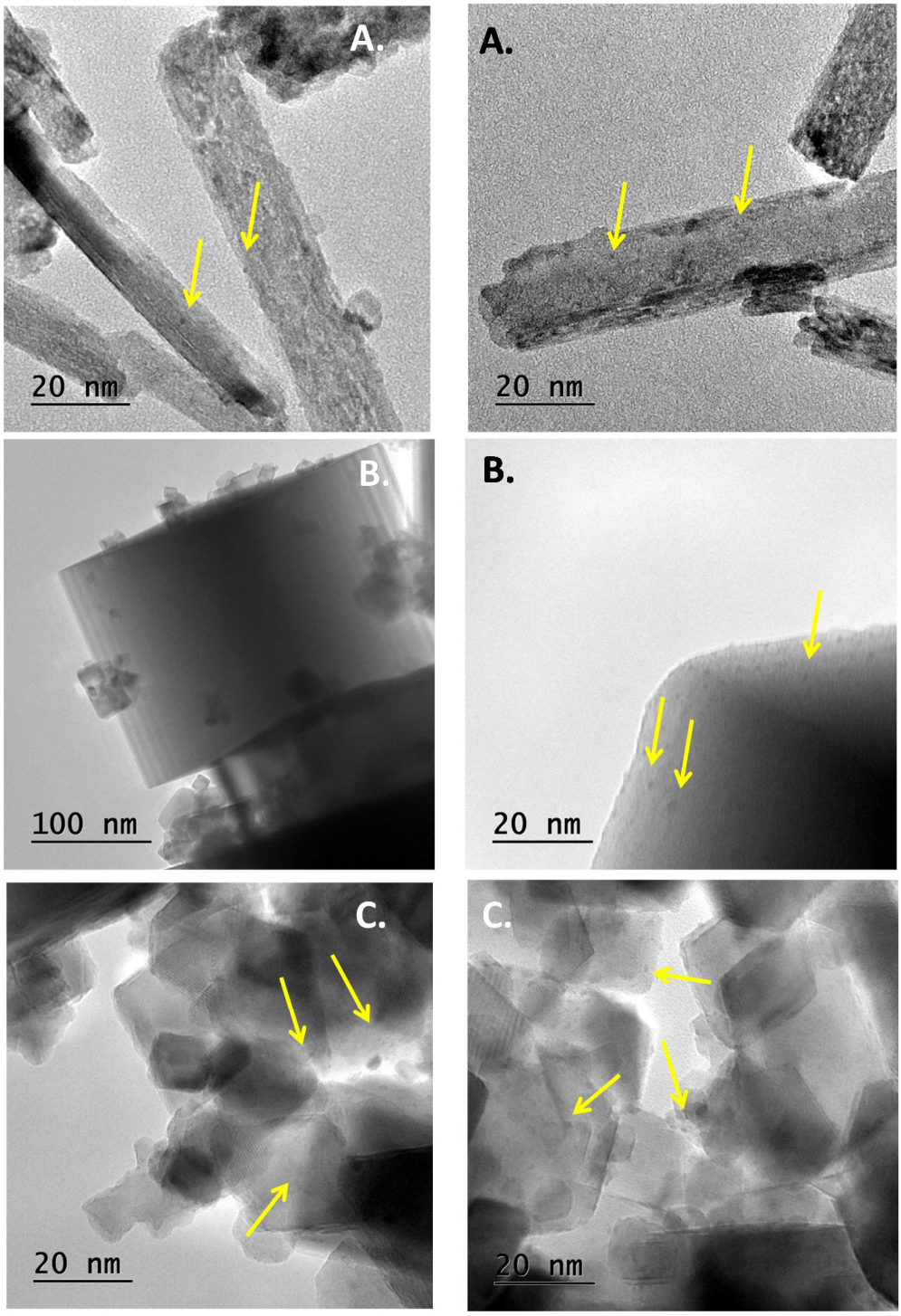

Figure 2: Representative TEM images of 1.5wt.% Pt supported on: A. CeO_2 nanorods B. CeO_2 nanocubes and C. CeO_2 nanoparticles

XRD patterns (SI, Figure 1) reveal the fluorite crystalline structure of the different ceria supports with no evidence of platinum diffraction peaks, which suggests an average platinum size <2 nm in agreement with the TEM characterisation. The superior activity of the Pt/CeO_2

nanorods is directly related to the constraints of the 1D (9.1 nm crystallite size and a 7 nm average diameter, Table 1) [21], while the larger crystallite size of the ceria nanocubes makes their re-oxidation by water more difficult [22], reducing its catalytic activity.

The average platinum particle size was estimated by CO pulse chemisorption at room temperature assuming hemispherical metal particles. The average particle size ranges from 0.8 nm in the 1.5wt.% Pt / CeO_2 particles to 1.0 nm in the 1.5wt.% Pt / CeO_2 rods and 1.5 nm in the 1.5wt.% Pt / CeO_2 cubes. It is likely that these metal particle sizes are underestimated due to the potential oxidation of CO to CO_2 using oxygen from the ceria in the presence of platinum. The catalytic activity of the different nanostructured catalysts can be in part due to the variation of the platinum particle size, despite the relatively small differences of mean values (ranging between 0.8 and 1.5 nm). The actual effect of the metal size is still argued in the literature. On one hand, it has been previously shown that the WGS reactivity is independent on platinum sizes < 2nm [23, 24], however, in-depth studies considering the length of periphery between Pt and ceria support clearly demonstrate the particle size – activity relationship [25]. Additionally, such relationships depend on the feed gas composition and reaction temperature.

Similar activation energy values between 45-50 kJ mol^{-1} (Table 1) are shown by all the Pt/CeO_2 catalysts calculated using the Arrhenius' plot (Figure 1B), where the specific rate values are calculated considering the overall amount of platinum in the catalysts. Calculations of the pre-exponential factor (A) reveal a considerably higher value for the Pt/CeO_2 rods catalysts, an order of magnitude higher than that presented by the cubes and particle counterparts. Consequently, a higher intrinsic kinetic constant is shown by the Pt/CeO_2 rods catalyst, directly related to the higher site reactivity in comparison to the Pt/CeO_2 particles and Pt/CeO_2 cubes.

Table 1 also presents the considerable higher reaction rate values (both per mass of catalysts and per total amount of platinum) at 275 ºC of the Pt/CeO_2 rods system respect to the other catalysts. Further characterisation is required to quantify the shape and size distribution of the

platinum particles to include their effect in the reaction rate comparison [25]. In any case, it is important to note that CO chemisorption analyses show that the 1.5%Pt/CeO_2 rods catalysts has an average particle size slightly bigger than platinum supported on CeO_2 particles and slightly lower than platinum supported on CeO_2 cubes, suggesting that the platinum-ceria support interaction has a more important effect in the resulting activity than the particle size (within the range studied, < 2nm).

Table 1: Physical properties and WGS reactivities of the different Pt/ CeO_2 catalysts

Catalyst	Surface area[a] / $m^2\ g^{-1}$	Crystal size[b] / nm	Reaction rate [c] / mol CO kg_{catal} h^{-1}	Specific rate [c] / mol CO mol_{Pt} h^{-1}	Activation Energy / kJ mol^{-1}	Pre-exponential factor (A) / h^{-1}	Intrinsic kinetic constant [c] / h^{-1}
1.5wt.% Pt / CeO_2 rods	74	9.1	189.8	2468	47.9	$1.1\cdot10^{8}$	$4.2\cdot10^{12}$
1.5wt.% Pt / CeO_2 cubes	13	37.3	43.1	561	46.1	$1.8\cdot10^{7}$	$6.1\cdot10^{11}$
1.5wt.% Pt / CeO_2 particles	144	4.5	49.9	650	49.4	$1.7\cdot10^{7}$	$8.9\cdot10^{11}$

[a] BET surface area measured by N_2 adsorption at 77 K.
[b] Average crystallite size from XRD patters using Scherrer equation.
[c] Measured at 275ºC.

Parallel formation of methane (via methanation) or even higher hydrocarbon molecules (via Fischer-Trospch) [26] decreases the hydrogen yield and can poison the anode catalyst in fuel cells. 1.5wt.%Pt/CeO_2 nanorods form methane at temperatures >250ºC while methane conversion decreases at temperatures above 375ºC due to the thermodynamic limitations associated to the WGSR, decreasing the formation of hydrogen and consequently of methane. Platinum supported on ceria particles and ceria cubes only produce methane at temperatures above 300ºC (Figure 3A). It is important to note, in order to facilitate the comparison to other studies, that CO relative conversion and methane selectivity normally increases as the H_2O/CO molar ratio increases.

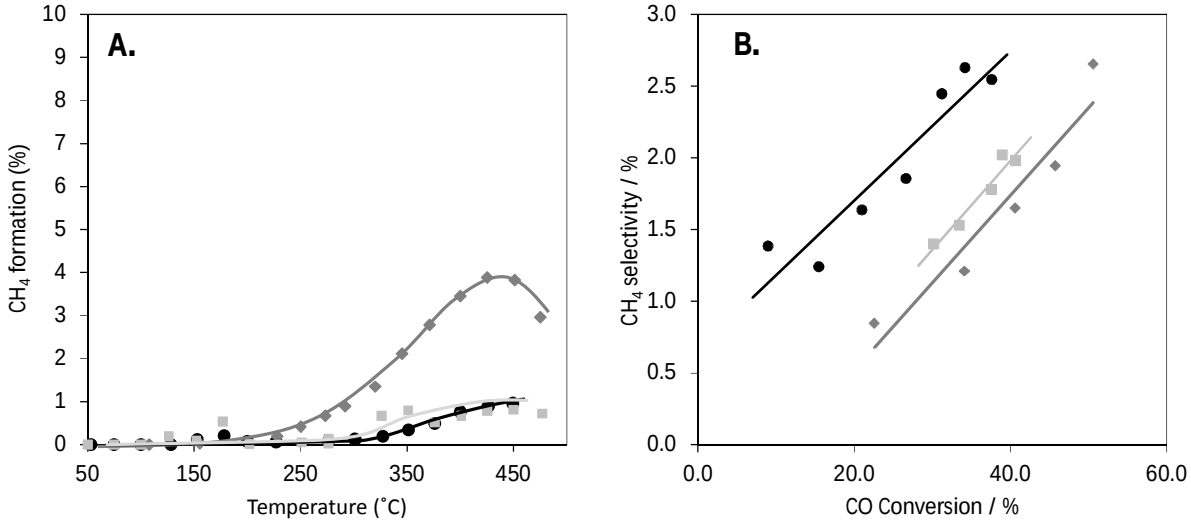

Figure 3: A. Methane formation and B. Relationship between CO conversion and CH_4 selectivity in the WGSR with 1.5wt.%Pt supported on ♦ CeO_2 nanorods ■ CeO_2 nanocubes ● CeO_2 nanoparticles

To facilitate the comparison between the different catalysts, Figure 3B shows the methane selectivity as a function of CO conversion. For the 1.5wt.% Pt/CeO_2 nanorods, only data under WGSR kinetic limitation (< 375 ºC) is used. In all cases, a linear relationship is observed, with the methane selectivity increasing as the CO conversion increases. Interestingly, this plot reveals that the 1.5wt.% Pt/CeO_2 nanorods is the most selective catalyst towards hydrogen production versus methane formation. On the other hand, 1.5wt.% Pt/CeO_2 nanocubes present the highest relative activity towards methane formation. As the undesirable formation of methane takes place on the metallic platinum surface, especially on the platinum atoms in contact with ceria [27], the difference on selectivity amongst the catalysts suggests variations on the Pt- CeO_2 interactions in the different catalysts as similar platinum particle sizes are present in all the catalysts as discussed above [28].

The platinum- CeO_2 interaction additionally affects the reducibility of the ceria support [11] which was assessed by consecutive temperature programme reduction analyses with an oxidation stage in between. Figure 4 shows the temperature programme reduction profiles, including the support-only for comparison.

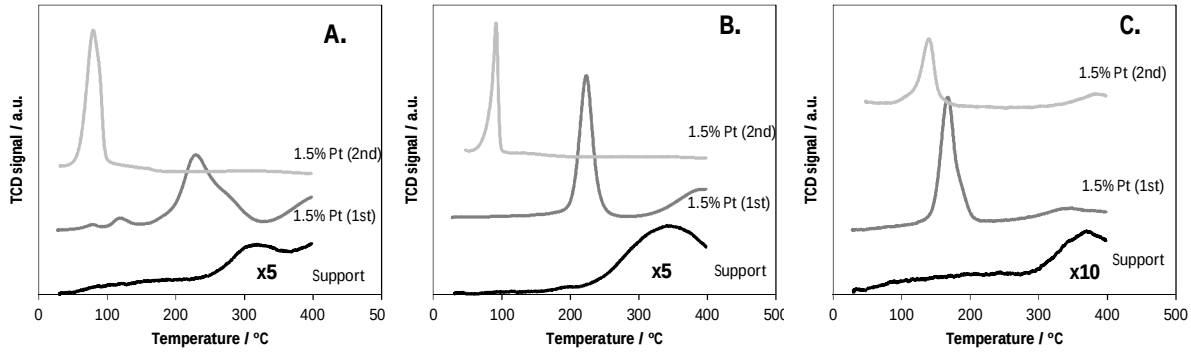

Figure 4: H_2-TPR cycles of A. 1.5wt.% Pt/ CeO_2 particles, B. 1.5wt.% Pt/ CeO_2 rods and C. 1.5wt.% Pt/ CeO_2 cubes. The H_2-TPR of the respective supports is shown for comparison. TPO up to 400 ºC was carried out between the 1st and 2nd TPR cycles.

In the first H_2-TPR cycle of the Pt/ CeO_2 catalysts, hydrogen consumption takes place predominately at temperatures between 150-250ºC. Platinum supported on ceria cubes reduce at lower temperatures than that supported on the ceria particles and rods what suggests a slightly higher metal particle size in agreement to the CO chemisorption calculations. In any case, the amount of hydrogen consumed (Table 2) is higher than that required for the reduction of Pt^{2+} to Pt^0 during the formation of the metal nanoparticles. In addition, the reduction peak of readily available oxygen (also called surface oxygen) of the ceria support is not present on the H_2-TPR of the Pt/ CeO_2 catalysts what confirms the weakening of the O-Ce bond by the presence of platinum facilitating the H_2 spill-over and the ceria reducibility at considerably lower temperatures as previously observed in the literature [10, 29].

Table 2: Reducibility of Pt supported on nanostructured ceria catalysts

Catalyst	TPR Cycle 1		TPR Cycle 2	
	T^a / ºC	H_2 consumption / μmol g^{-1}	T^a / ºC	H_2 consumption / μmol g^{-1}
1.5wt.% Pt / CeO_2 rods	220	7317	90	2877
1.5wt.% Pt / CeO_2 cubes	156	1011	135	548
1.5wt.% Pt / CeO_2 particles	222	5410	77	4297

[a] Peak temperature of the main reduction peak

After oxidation of the catalysts at 400ºC, a second TPR cycle was carried out where a sharper reduction peak at lower temperatures is observed for the three Pt/ CeO_2 systems. Additionally, the hydrogen consumption decreases in a similar order of magnitude than that reported for different Pt/ CeO_2 catalysts [30], suggesting the presence of carbonates or formates on the fresh catalysts after metal loading which are removed during the first TPR. Consecutive TPR cycles are similar to the second one. It is important to highlight that the potential presence of formates and carbonates does not affect our WGSR activity data as the catalysts are pre-reduced prior the catalytic tests, having such groups removed from the surface of the catalysts. In any case, the hydrogen consumption is higher than the amount required for the reduction of Pt^{2+} to Pt^0 but relatively small in the case of the 1.5wt.% Pt/CeO_2 nanocubes. This catalyst shows an additional reduction peak at temperatures ~350ºC, similar to the one characteristic for the reduction of surface oxygen in the ceria nanocubes support (Figure 4C) which suggests a lower H_2 spill-over due to poorer platinum-ceria interaction on the selectively exposed (100) plane. This poor metal-support interaction is believed to be related to the poor hydrogen yield and relatively high methane formation of the 1.5 wt.% Pt/CeO_2 nanocubes catalyst with respect to the other ones [27]. Contrary, ceria nanorods with selective exposure of the (110) and (100) crystal planes are shown to provide an optimum platinum-ceria interaction compared to the (111) and (100) crystal planes exposed in the ceria nanoparticles. This observation is in agreement with theoretical calculations of gold clusters supported on ceria catalysts where the WGS reaction is preferred on the CeO_2 (110) surface over the CeO_2 (111) one because of the lower binding energy of OH on the former surface [31]. In addition, the (110) and (100) planes present in the ceria nanorods enhanced the re-oxidation of the ceria with respect to its particles and cubes counterparts, as previously shown in the oxidation reactions in the absence of metal nanoparticles [17, 20], playing a key role on the catalytic cycle of the WGSR. Additionally,

recent theoretical and experimental studies of Ni/CeO_2 systems reveal the enhancement effect of the presence of strongly bonded Ni on the ability of ceria to dissociate water, an intermediate step related to the re-oxidation of ceria in the WGSR catalytic cycle [32].

Conclusions

A series of 1.5wt.% Pt/ CeO_2 catalysts were synthesised by a single metal loading method (incipient wetness impregnation) on different nanostructured ceria supports. Their catalytic behaviour on the WGSR demonstrates that the nanostructured morphology of the ceria support and the exposed crystal planes play a crucial role on the resulting catalytic activity and selectivity. The 1.5wt.% platinum supported on ceria nanorods present the highest catalytic activity and lower methane selectivity associated to the selective exposure of the (110) crystal plane. Additionally the relatively poor platinum-ceria nanocubes interaction is translated into a low activity and high methane selectivity.

Acknowledgments

The authors would like to acknowledge EPSRC (grant number EP/L020432/1) for funding, and the Research Catalysis Group at Harwell (RCaH) for access to the TEM microscopy facilities.

References

1. Twigg, M.V., *Catalyst Handbook*. Second ed. 1989: Wolfe Publishing Ltd.
2. Song, C.S., *Fuel processing for low-temperature and high-temperature fuel cells - Challenges, and opportunities for sustainable development in the 21st century.* Catalysis Today, 2002. **77**(1-2): p. 17-49.
3. Ghenciu, A.F., *Review of fuel processing catalysts for hydrogen production in PEM fuel cell systems.* Current Opinion in Solid State & Materials Science, 2002. **6**(5): p. 389-399.
4. Trimm, D.L. and Z.I. Onsan, *Onboard fuel conversion for hydrogen-fuel-cell-driven vehicles.* Catalysis Reviews-Science and Engineering, 2001. **43**(1-2): p. 31-84.
5. Pena, M.A., J.P. Gomez, and J.L.G. Fierro, *New catalytic routes for syngas and hydrogen production.* Applied Catalysis a-General, 1996. **144**(1-2): p. 7-57.
6. Ratnasamy, P. and S. Sivasanker, *STRUCTURAL CHEMISTRY OF CO-MO-ALUMINA CATALYSTS.* Catalysis Reviews-Science and Engineering, 1980. **22**(3): p. 401-429.

7. Gonzalez, I.D., et al., *A comparative study of the water gas shift reaction over platinum catalysts supported on CeO2, TiO2 and Ce-modified TiO2.* Catalysis Today, 2010. **149**(3-4): p. 372-379.
8. Meunier, F.C., et al., *Quantitative DRIFTS investigation of possible reaction mechanisms for the water-gas shift reaction on high-activity Pt- and Au-based catalysts.* Journal of Catalysis, 2007. **252**(1): p. 18-22.
9. Garcia-Garcia, F.R., et al., *Hollow fibre membrane reactors for high H-2 yields in the WGS reaction.* Journal of Membrane Science, 2012. **405**: p. 30-37.
10. Yao, H.C. and Y.F.Y. Yao, *CERIA IN AUTOMOTIVE EXHAUST CATALYSTS .1. OXYGEN STORAGE.* Journal of Catalysis, 1984. **86**(2): p. 254-265.
11. Fu, Q., H. Saltsburg, and M. Flytzani-Stephanopoulos, *Active nonmetallic Au and Pt species on ceria-based water-gas shift catalysts.* Science, 2003. **301**(5635): p. 935-938.
12. Yeung, C.M.Y., et al., *Engineering Pt in ceria for a maximum metal-support interaction in catalysis.* Journal of the American Chemical Society, 2005. **127**(51): p. 18010-18011.
13. Mei, Z.J., et al., *Effect of the interactions between Pt species and ceria on Pt/ceria catalysts for water gas shift: The XPS studies.* Chemical Engineering Journal, 2015. **259**: p. 293-302.
14. Cordatos, H., D. Ford, and R.J. Gorte, *Simulated annealing study of the structure and reducibility in ceria clusters.* Journal of Physical Chemistry, 1996. **100**(46): p. 18128-18132.
15. Petallidou, K.C., C.M. Kalamaras, and A.M. Efstathiou, *The effect of La3+, Ti4+ and Zr4+ dopants on the mechanism of WGS on ceria-doped supported Pt catalysts.* Catalysis Today, 2014. **228**: p. 183-193.
16. Petallidou, K.C. and A.M. Efstathiou, *Low-temperature water-gas shift on Pt/Ce1-xLaxO2-delta: Effect of Ce/La ratio.* Applied Catalysis B-Environmental, 2013. **140**: p. 333-347.
17. Torrente-Murciano, L., et al., *Shape-dependency activity of nanostructured CeO2 in the total oxidation of polycyclic aromatic hydrocarbons.* Applied Catalysis B: Environmental, 2013. **132–133**(0): p. 116-122.
18. Mann, A.K.P., et al., *Adsorption and Reaction of Acetaldehyde on Shape-Controlled CeO2 Nanocrystals: Elucidation of Structure-Function Relationships.* Acs Catalysis, 2014. **4**(8): p. 2437-2448.
19. Vile, G., et al., *Opposite Face Sensitivity of CeO2 in Hydrogenation and Oxidation Catalysis.* Angewandte Chemie-International Edition, 2014. **53**(45): p. 12069-12072.
20. López, J.M., et al., *The prevalence of surface oxygen vacancies over the mobility of bulk oxygen in nanostructured ceria for the total toluene oxidation.* Applied Catalysis B: Environmental, 2015. **174–175**(0): p. 403-412.
21. Sayle, T.X.T., et al., *Strain and Architecture-Tuned Reactivity in Ceria Nanostructures; Enhanced Catalytic Oxidation of CO to CO2.* Chemistry of Materials, 2012. **24**(10): p. 1811-1821.
22. Bunluesin, T., R.J. Gorte, and G.W. Graham, *Studies of the water-gas-shift reaction on ceria-supported Pt, Pd, and Rh: implications for oxygen-storage properties.* Applied Catalysis B-Environmental, 1998. **15**(1-2): p. 107-114.
23. Panagiotopoulou, P. and D.I. Kondarides, *Effect of the nature of the support on the catalytic performance of noble metal catalysts for the water-gas shift reaction.* Catalysis Today, 2006. **112**(1-4): p. 49-52.
24. Tiwari, R., et al., *Pt nanoparticles with tuneable size supported on nanocrystalline ceria for the low temperature water-gas-shift (WGS) reaction.* Journal of Molecular Catalysis a-Chemical, 2014. **395**: p. 117-123.
25. Kalamaras, C.M., S. Americanou, and A.M. Efstathiou, *"Redox" vs "associative formate with -OH group regeneration" WGS reaction mechanism on Pt/CeO2: Effect of platinum particle size.* Journal of Catalysis, 2011. **279**(2): p. 287-300.
26. Torrente-Murciano, L., et al., *Formation of hydrocarbons via CO2 hydrogenation – A thermodynamic study.* Journal of CO2 Utilization, 2014. **6**(0): p. 34-39.
27. Yeung, C.M.Y. and S.C. Tsang, *Noble Metal Core-Ceria Shell Catalysts For Water-Gas Shift Reaction.* Journal of Physical Chemistry C, 2009. **113**(15): p. 6074-6087.
28. Aranifard, S., S.C. Ammal, and A. Heyden, *On the importance of metal-oxide interface sites for the water-gas shift reaction over Pt/CeO2 catalysts.* Journal of Catalysis, 2014. **309**: p. 314-324.

29. Ivanov, I., et al., *Comparative Study of Ceria Supported Nano-sized Platinum Catalysts Synthesized by Extractive-Pyrolytic Method for Low-Temperature WGS Reaction.* Catalysis Letters, 2013. **143**(9): p. 942-949.
30. Pierre, D., W.L. Deng, and M. Flytzani-Stephanopoulos, *The importance of strongly bound Pt-CeOx species for the water-gas shift reaction: Catalyst activity and stability evaluation.* Topics in Catalysis, 2007. **46**(3-4): p. 363-373.
31. Song, W.Y. and E.J.M. Hensen, *Mechanistic Aspects of the Water-Gas Shift Reaction on Isolated and Clustered Au Atoms on CeO2(110): A Density Functional Theory Study.* Acs Catalysis, 2014. **4**(6): p. 1885-1892.
32. Carrasco, J., et al., *In Situ and Theoretical Studies for the Dissociation of Water on an Active Ni/CeO2 Catalyst: Importance of Strong Metal-Support Interactions for the Cleavage of O-H Bonds.* Angewandte Chemie-International Edition, 2015. **54**(13): p. 3917-3921.